Microfluidic technologies: buffer exchange in bioprocessing, a mini review

Microfluidics and Nanofluidics (2024) 28:79
https://doi.org/10.1007/s10404-024-02775-3

REVIEW

Microfluidic technologies: buffer exchange in bioprocessing, a mini review

Tom Carvell[1] · Paul Burgoyne[2] · Alasdair R. Fraser[2,3] · Helen Bridle[1]

Received: 23 September 2024 / Accepted: 19 November 2024

Abstract
Buffer exchange is a common process in manufacturing protocols for a wide range of bioprocessing applications, with a variety of technologies available to manipulate biological materials for culture medium exchange, cell washing and buffer removal. Microfluidics is an emerging field for buffer exchange and has shown promising results with both prototype research and commercialised devices which are inexpensive, highly customisable and often have the capacity for scalability to substantially increase throughput. Microfluidic devices are capable of processing biological materials and exchanging solutions without the need for conventional processing techniques like centrifugation, which are time-consuming, unsuitable for large volumes and may be damaging to cells. The use of microfluidic separation devices for cell therapy manufacturing has been under-explored despite some device designs successfully being used for diagnostic enrichment of rare circulating tumour cells from peripheral blood. This mini-review aims to review the current state of microfluidic devices for buffer exchange, provide an insight into the advantages microfluidics offers for buffer exchange and identify future developments key to exploiting the technology for this application.

1 Introduction

The recent introduction of advanced therapeutic medicinal products to cancer treatment and regenerative medicine has had a substantial contribution to patient health, but faces significant challenges in manufacture as they are based on the use of living cells rather than drugs or biomolecules. These cell-based treatments generally require complex manufacturing procedures to go from source material through to their final formulation (Weber et al. 2020). Regenerative cell therapies involve one or more stages including the isolation, expansion, manipulation and infusion of target cells to restore or improve the function of damaged tissues or organs within the body. This is mediated by utilising the unique properties of various types of cells to promote healing, repair injured tissues, or replace dysfunctional cells (Brown et al. 2019; El-Kadiry et al. 2021; Koo 2024; Moroni et al. 2019; Starkey Lewis et al. 2019). Other cell therapies include immune-based therapies for cancer treatment, harnessing the anti-tumour effects of T cells, NK cells and other lymphocytes (Cooper et al. 2024; Myers and Miller 2021; Roddie et al. 2019). Additionally there are antibody-based therapies that are comprised of large complexes of proteins that require multi-step purification from the starting materials (R.-M. Lu et al. 2020). Throughout their manufacturing processes, both cell (Fig. 1), and antibody-based therapies require buffer exchange to remove unwanted ions, small molecules, or waste products and contaminants from the final formulation delivered to patients (Elverum and Whitman 2020; Kurnik et al. 1995). Whilst this review contains devices used for the buffer exchange of molecules, a focus is placed on devices whose function can be extended to processing cells.

Figure 1 is a schematic diagram illustrating an example of an autologous stem cell therapy manufacturing process where patient cells undergo genetic modification before they are reinfused back into the patient. It highlights the

✉ Tom Carvell
trc2000@hw.ac.uk

[1] Institute of Biological Chemistry, Biophysics and Bioengineering, School of Engineering and Physical Sciences, Heriot-Watt University, Heriot-Watt Research Park, Currie EH14 4AS, UK

[2] Tissues, Cells and Advanced Therapeutics, Jack Copland Centre, Scottish National Blood Transfusion Service, Research Avenue North, Heriot-Watt Research Park, Edinburgh EH14 4BE, UK

[3] Swarm Oncology Ltd., 15 Stukeley Street, London WC2B 5LT, UK

Published online: 27 November 2024

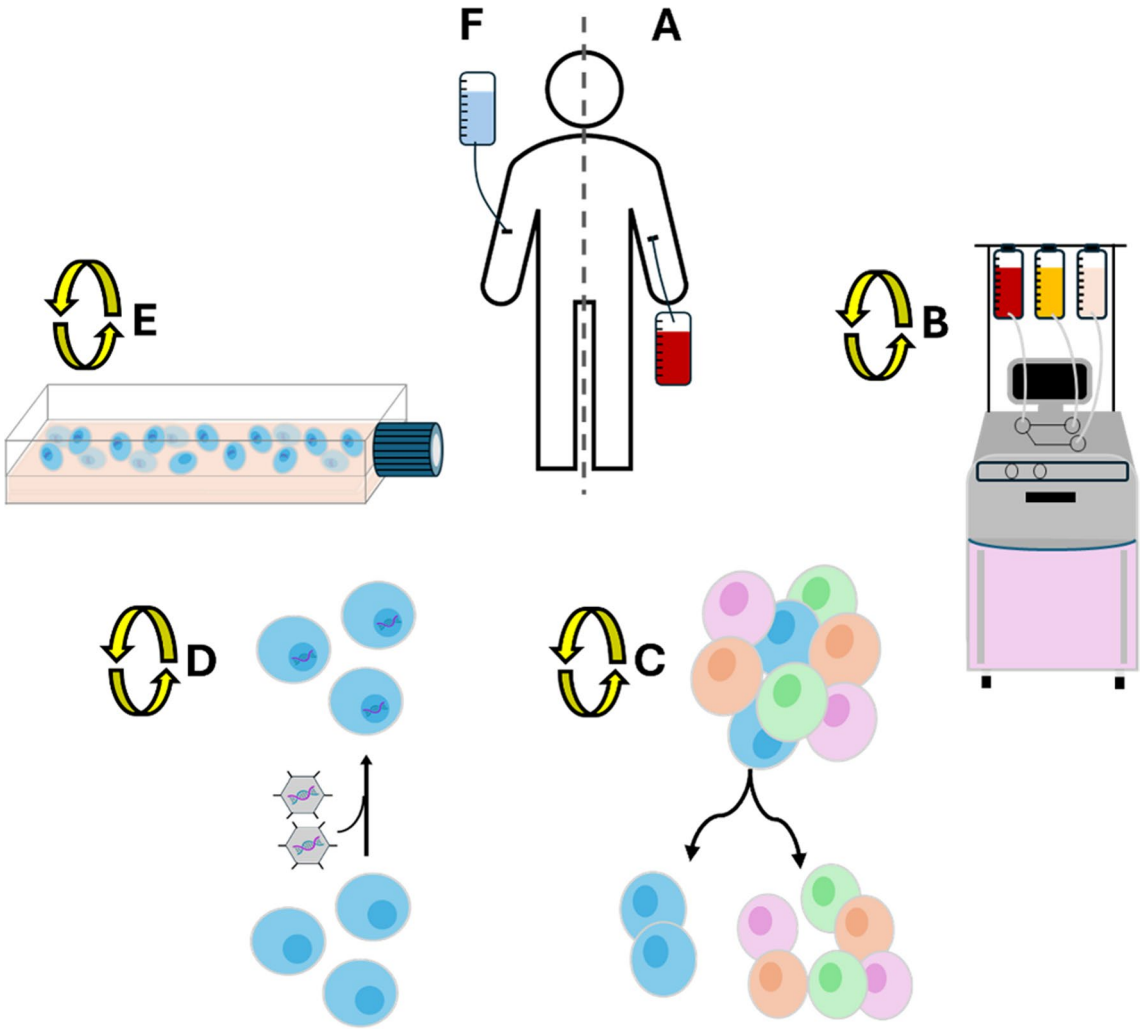

Fig. 1 An example of the basic outline of a stem cel-based cell therapy manufacturing process and the importance of buffer exchange. **A**) The patient donates blood which can be **B**) processed by an apheresis machine so that the leukocyte component is separated from the rest of the peripheral blood before the **C**) target haematopoietic stem cells are isolated and non-target cells are discarded. **D**) Isolated target cells may undergo genetic modification before **E**) culturing and are harvested before **F**) the cell therapy product is reinfused back to the patient. Buffer exchange (yellow curved arrows) is required throughout the manufacturing process

importance of buffer exchange within the manufacturing process due to the numerous times that changing the fluid environment of cells is required. Furthermore, devices capable of precise, repeatable, and efficient buffer exchange have the potential to be utilised as part of more complex biotechnological processes.

Buffer exchange refers to the process of replacing the solution that contains a biological sample with an alternative buffer solution and this is often performed to alter the fluid environment of the sample to allow for subsequent experimental, expansion, storage or analytical processes (Li et al. 2019; Madariaga-Marcos et al. 2020; VanAernum et al. 2020; Yang et al. 2024). Efficient and effective buffer exchange is critical for the successful manufacturing of cell therapies (Lu et al. 2019) such as chimeric antigen receptor T cell therapies (Vormittag et al. 2018). The manufacturing processes often utilise an approach summarised by target cell isolation and purification before transferring material back into the patient.

To achieve this, various technologies exist to isolate cells through the use of labels including antibody-based fluorescence-activated cell sorting (FACS) or magnetic-activated cell sorting (MACS), as well as cell-ligand binding (Tomlinson et al. 2013). Whilst FACS and MACS are both powerful for the sorting and isolation of specific cell populations, there is a lack of Good Manufacturing Practice (GMP)-compliant sorting reagents for many cell surface receptors and also the potential for post-processing cell activation. To enable solution exchange for purification and culturing during the manufacturing process, other label-free technologies include devices that utilise centrifugation, filtration or sedimentation. These non-microfluidic based methods of buffer

Table 1 Examples of conventional bioprocessing technologies

Bioprocessing technology	Use of labelling	Batch or continuous	Performance	Throughput	Reference
Manual centrifugation	No label	Batch	~97% plasma removal[1]	Variable[1]	(Iwama et al. 2017)
Automated centrifugation (e.g. ACP 215)	No label	Batch	~99% plasma removal	Up to $\sim 1.3 \times 10^{10}$ red blood cells/minute	(Iwama et al. 2017; Oikawa et al. 2016)
Magnetic-activated cell sorting systems	Label	Batch	Recovery of up to 91–93% of target cells	Variable, but tested with 8×10^6 cells per process	(Sutermaster and Darling 2019)
Fluorescent-activated cell sorting systems	Label	Batch	Recovery of up to 30% of target cells	Variable, but tested with 8×10^6 cells per process	(Cossarizza et al. 2017; Sutermaster and Darling 2019)
Filtration-based (Cytomate)	No label	Batch	~75% cell recovery, 96% removal of DMSO.	Variable, but 1 h processing time.	(Calmels et al. 2003)
Filtration-based (Lovo)	No label	Batch	~90% cell recovery	Variable, but up to 3.33×10^6 cells/minute.	(Ibenana et al. 2022)
Sedimentation-based (e.g. BioSep)	No label	Continuous	Up to 99% cell recovery.	Variable, but the largest system is capable of processing up to ~700mL/minute.	(BioSep 2020; Li et al. 2021)

[1] This is variable due to manual operation and the data is quoted from one study when in comparison with automated centrifuge technologies such as ACP 215

Table 2 Advantages and disadvantages of microfluidic devices

Advantages	Disadvantages
Small sample volumes	Challenges with scalability
Simplicity of operation	Complexity of design
Reproducibility	Predicting flow parameters
Low-cost	Complexity of fabrication
Potential for extremely high throughput	Surface effects
Closed system integration	Clogging of microchannels
Portability	Limited material options
Small laboratory footprint	Non-standardised

exchange of cells (Li et al. 2021; Lu et al. 2019) have been effectively reviewed elsewhere. Whilst these different technologies are employed for a variety of applications, Table 1 describes application-specific performances, and throughputs, to enable a better comparison between devices.

The final practical stage of administering a cell therapy administration frequently involves the transplantation of frozen cells back into the patient. It is essential that these processes are gentle but perform fast solution exchange post-thaw to avoid sensitive cells spending prolonged periods of time in a suboptimal fluid environment, or causing damage to target cells through shear forces associated with other volume reduction methods.

Whilst this review paper aims to evaluate microfluidic devices capable of buffer exchange within biotechnologies, a particular focus has been placed on devices used for cell processing. Microfluidic devices have not been widely adopted for buffer exchange and centrifugation remains the most common conventional method when used for applications involving cells, but many more technologies have emerged for the buffer exchange of both cells and proteins. As with every type of technology, microfluidic devices have their disadvantages, but they have several key advantages relative to conventional methods of buffer exchange (Table 2) (Bahnemann and Grünberger 2022; Battat et al. 2022; Convery and Gadegaard 2019).

Whilst Table 2 details the general advantages and disadvantages of microfluidic devices, some buffer exchange specific microfluidic devices share the advantage of centrifugation in being label-free, and therefore do not require subsequent processing to purify cells and remove contaminants (Carvell et al. 2024). In conventional manual batch-based centrifugation-based processors the biological material undergoes pelletisation in one buffer and resuspension of the pelleted cells into another, whereas microfluidic devices offer an opportunity for continuous bioprocessing, avoiding the potential cell damage associated with these two processes (Delahaye et al. 2015). In a recent study by Carvell et al., inertial microfluidic processing of leukocytes demonstrated no significant differences in the cell viability, in comparison with conventional batch centrifuge (Carvell et al. 2024). Despite the huge potential for compact scalability relative to most bioprocessing technologies, microfluidic devices may not reach the same throughput and scalability of bioprocessing when compared with continuous centrifuge alternatives (Masri et al. 2017). However, microfluidic devices are versatile in design, and more easily accessible for resource-restricted research laboratory environments (Lu et al. 2019). Additionally, microfluidics enable biological material to be manipulated based on the size and shape of the target material alone (Kalyan et al. 2021) and thus continuous separation of cells based on varying characteristics such as deformability (Guzniczak et al. 2020). As the channels are at the microscale (i.e. smaller than a millimetre in dimension), clogging has been a major hurdle for

large-scale adoption of microfluidic-based bioprocessors (Kersaudy-Kerhoas and Sollier 2013) but has reportedly been overcome in some devices using microresistor-generated thermal vapour bubbles to clear debris from microchannels (Pritchard et al. 2019).

These microfluidic devices, ranging from simple passive systems to intricate active devices, offer precise control over fluid flow and composition at the microscale. By examining the design principles, operational mechanisms, and performance characteristics of these devices, we aim to provide an insight into the potential for their applicability in a diverse range of research and industrial settings within advanced therapy manufacturing processes.

2 Methods

Although this review aims to provide a summary of microfluidic devices used in buffer exchange, this is not an exhaustive list and examples of devices have been provided. It is possible that devices in other reports perform buffer exchange during bioprocessing, but as the buffer exchange was not a primary endpoint, this was not detailed by the authors. Literature searches using PubMed and Google Scholar were performed during April and June 2024 using the following search terms: 'buffer exchange microfluidics', 'reagent exchange microfluidics', 'solution exchange microfluidics', 'medium exchange microfluidics'. The searches resulted in hundreds of publications from 2008 to 2024, and a focus was placed on those used for processing of cells and those reporting in the last decade; subsequently the abstracts were used to determine inclusion into the article. Inclusion criteria was based on perceived novelty, throughput, performance, and the intended application.

3 Outcomes

Overall, 23 relevant microfluidic devices were identified from the literature search, comprising 12 relying on the passive approach of inertial focusing, 3 using deterministic lateral displacement (DLD), 2 using hydrodynamic filtration and 3 using active methods like dielectrophoresis (DEP). Two other devices were also included that utilise less conventional microfluidic technologies. Details of the different approaches and example devices are discussed below. As a summary, Fig. 2 shows the relationship between normalised processing rate and device performance (as a percentage of maximal outcome, where 100% reflects complete buffer exchange) of microfluidic devices used for buffer exchange as listed in Table 3. For the devices numbered 12 and 22 (Table 3), an arbitrary 100% performance was awarded

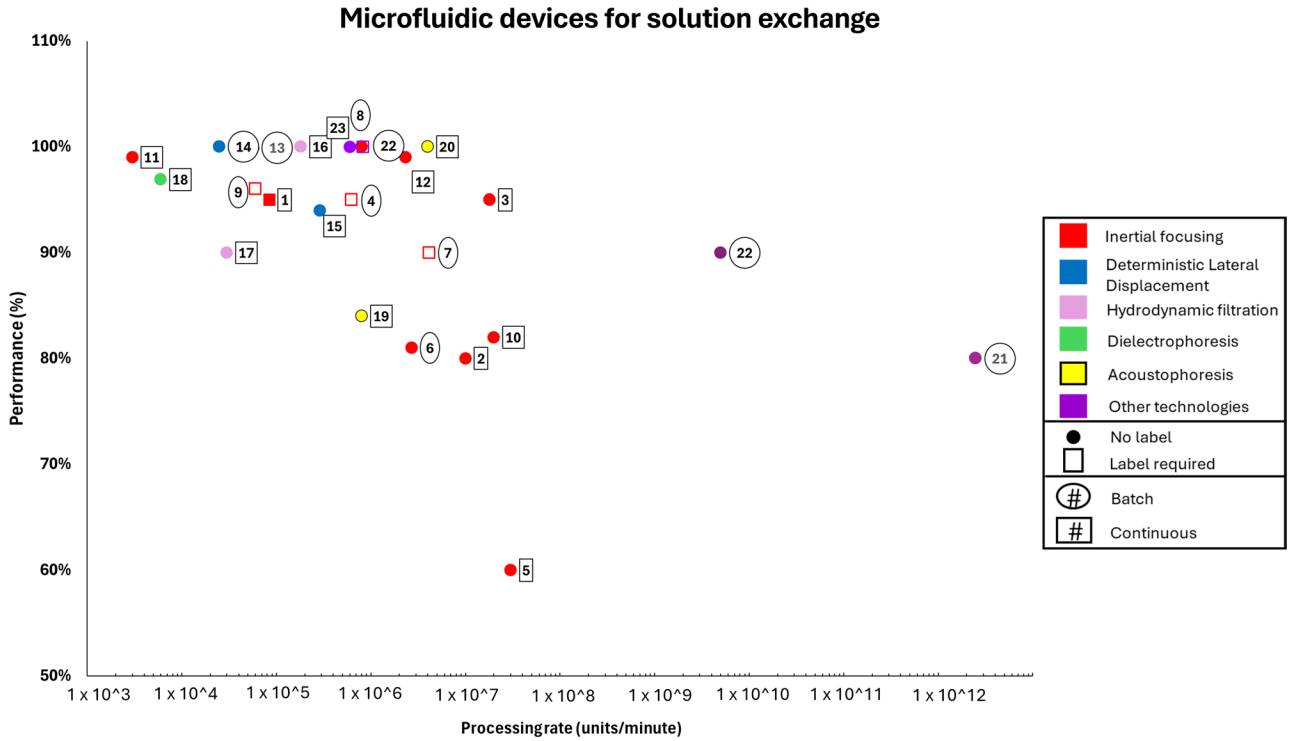

Fig. 2 The relationships between device performance, processing rate, device type, label use and continuous or batch processing. Colour indicates device type. Marker type indicates use of labelling during processing. Numbering refers to numbered order in Table 3, and shape outline indicates batch or continuous processing. Processing rate of units/minute refers to biological components (such as cells) processed per minute. Performance percentage refers to capacity to achieve maximal performance for a given application

as the device performed buffer exchange successfully for their application, but no quantifiable data were generated. The processing rate refers to the number of units processed per minute, for example the number of cells or exosomes (membrane bound extracellular vesicles) that underwent buffer exchange per minute. Some studies did not report the performance of buffer exchange as it was not a main outcome of the experiment and were excluded from the analysis. Whether a device could feasibly be used in continuous bioprocessing and any labelling requirements for successful buffer exchange are also detailed.

A range of microfluidic device types were identified and schematic diagrams depicting their function is provided in Fig. 3. In the outcomes section below, devices are ordered primarily by type of microfluidic device and secondly, by performance.

4 Inertial focusing and Dean flow

Inertial focusing (IF) refers to the phenomenon whereby particles or cells suspended in a fluid are directed towards specific equilibrium positions within a microchannel. As the fluid flows through the microchannel, the inertia of the particles causes them to migrate towards distinct locations within the channel cross-section based on properties such as size and density. This migration is influenced by inertial lift forces, which push the particles towards the channel walls, and wall-induced shear forces, which push them towards the channel centre. Ultimately, equilibrium between these forces results in the particles forming ordered streams or layers within the fluid flow. Inertial focusing is utilized in various microfluidic applications for particle separation, cell sorting, and precise manipulation of particles or cells within microchannels (Amini et al. 2014; Huang et al. 2020; Martel and Toner 2014). Dean flow coupled IF occurs in curved microchannels where fluid flow experiences secondary Dean vortices due to centrifugal forces generated by the microchannel geometry. As the flow progresses through the curved channels, the combined effects of Dean flow and inertial forces induces particles to migrate towards distinct lateral equilibrium positions, resulting in their focusing at specific locations. Flow rate, channel curvature, and particle size collectively influence the strength and extent of Dean flow-induced lateral migration (Gou et al. 2018; Ramachandraiah et al. 2014).

Both IF and Dean flow operate within laminar flow regimes whereby fluids move smoothly and orderly in parallel layers, with minimal disruption between adjacent layers. This orderly flow arises due to the dominant influence of viscous forces over inertial forces. Unlike turbulent flow, where chaotic motion leads to thorough mixing of fluids, laminar flow maintains distinct layers that flow without significant intermixing. The absence of turbulence prevents the transfer of momentum and mass between adjacent fluid layers, resulting in a lack of mixing. Even when different fluids are introduced into laminar flow conditions, they typically remain in separate, distinct layers without significant blending. Consequently, the injection of two buffers into the microchannels of Dean flow coupled-IF devices can lead to the transfer of particles or cells across streamlines and can be used to facilitate buffer exchange through hydrodynamic forces alone, in a label-free and centrifugation-free processing step (Huang et al. 2020; Kalyan et al. 2021).

Numerous microfluidics devices with a range of designs have been reported to utilise IF and Dean flow for buffer exchange with varying performances. Although it was not a primary outcome of the study by Ouyang et al., adequate buffer exchange was achieved using an IF device to facilitate the electroporation of various cell types. This assumption is made because the composition of the buffer is critical for successful electroporation. The device used IF but solution exchange was performed via multiple solution injection ports and demonstrated a capacity to perform electroporation with high efficiency and therefore was an ideal tool for the intracellular delivery of multiple biomolecules. The device appears less suitable for buffer exchange in applications other than the electroporation of cells as the device utilises a small chamber for solution exchange and scale up for other applications could prove challenging (Ouyang et al. 2017).

Another IF device reported as performing buffer exchange was comprised of 2 inlets into straight channels and vortex-inducing chambers leading to 4 outlets. A mixture of human cancer stem-like cells (HuSLCs)(1000/mL) and diluted blood (1%) was injected into the device at ~300µL/min. The cells underwent IF and aligned based on their physical properties and as they entered the first vortex-inducing chamber the larger cells exited the into the sheath flow and were collected at the side outlets. Some smaller, non-target cells were also transferred to the sheath flow where they were recycled to a second vortex-inducing chamber and the process repeated leading to continuous bioprocessing with a separation efficiency of 90% and an 1500 fold increase in the purity of HuSLCs (Wang et al. 2016).

Another microfluidic device was reportedly designed to utilise IF and hydrodynamic resistance for exchange sample buffer prior to dielectrophoresis. Dielectrophoresis (discussed later in this review) requires buffer medium with a lower conductivity and this device was designed so that red blood cells ($\sim 4 \times 10^8$ /mL) in 1x phosphate buffered saline (PBS) were swapped into a buffer comprised of an 8% sucrose solution in water. As an excess of sucrose solution was used, side channel outlets were employed

Table 3 Microfluidic device used for buffer exchange in biotechnologies. The table lists materials used in fabrication, performance, throughput, targets, and other relevant details

Number	Device material(s)	Fabrication technique(s)	Microchannel architecture	Microchannel dimensions	Throughput	Performance	Application	Notes/ unique features	Reference
Inertial focusing and/or Dean-coupled flow device									
1	PDMS and glass	Soft lithography	Varies. Straight and wide, followed by asymmetric curved, straight and narrow, and expansion	Straight and wide: 80 µm width, curved: 40–180 µm width, straight and narrow: 20 µm width, all had 35 µm height.	2×10^6 cells/mL, fluid velocity of 0.5 m/s. +	88% solution exchange (3 passes), 95% (4 passes).	Removal of Eosin Y dye from cell suspension.	Staged device with multiple channel architectures	(Reece et al. 2015)
2	Plastic tubing with membrane-hydrogel composite, PDMS.	Unique assembly technique (unnamed).	Spiral architecture with 3 bifurcations along the tubing.	Main flow channel comprised of plastic tubing 22 m in length with an internal diameter of 1.02 mm.	50mL sample of haematocrit 10–15%. Flow rate varies but 300mL/hour was optimal.	Similar cell recovery but 5x lower concentration relative to centrifugation-based process.	Reduction of IgA in stored red blood cells.	Technically not microfluidics due to size of channel but device function is mediated via inertial focusing, a phenomenon frequently utilised within microfluidic devices.	(Vörös et al. 2018)
3	Resin (M2S-HT90 cures to polyacrylate)	Multijet 3D printing	Spiral architecture connected to buffer device and peristaltic pumps.	Microchannel length: 372 mm, width: 0.6 mm, height: 0.2 mm.	2×10^7 cells/mL at 0.5-1.3mL/min.	Separation efficiency of up to 95%.	Bioreactor recirculation.	Used with CHO cells. Old buffer discarded and cells recirculated to reactor.	(Enders et al. 2021)
4	PDMS, glass.	Soft lithography.	Spiral architecture, 2 inlets, 2 outlets.	Microchannel width: 500 µm, height: 115 µm.	10^5-10^6 cells/mL, co-flow of 1-1.5mL/min.	Performance evaluated through quantification of cells and (absence of) nanoparticles in outlet samples. 95% depletion of nanoparticles and > 90% cell recovery.	Separation of particles and cells with a solution exchange step.	Used with MSCs or THP-1. Requires labelling of cells. Continuous operation.	(Tay et al. 2016)
5	PMMA, SU-8.	Photolithography and laser ablation.	Spiral architecture, 2 inlets, 2 outlets.	Microchannel width: 480 µm, height: 80 µm, length: 220 mm.	2×10^6 cells/mL and ~15mL/min.	~60% buffer, 97% cell separation.	One step cell separation and solution exchange.	Used with peripheral blood mononuclear cells and monocytes.	(Carvell et al. 2024)

Table 3 (continued)

Number	Device material(s)	Fabrication technique(s)	Microchannel architecture	Microchannel dimensions	Throughput	Performance	Application	Notes/ unique features	Reference
6	PDMS, glass, SU-8.	Soft lithography.	Wavy microchannel architecture. 2 inlets, 3 trifurcated outlets.	Microchannel width: 40 µm, height: 10 µm, length: 10–30 mm	Particle sizes: 100 nm–1 µm. Typically, 6×10^7/mL. 44.9µL/min.	81% exosome of interest separation with 95% outlet purity.	Submicron particle and exosome separation prototype device.	Non-Newtonian fluid, polyethylene oxide solution and breast cancer culture medium exchange.	(Zhou et al. 2019)
7	PDMS, glass, SU8-2025.	Soft lithography.	Straight channel. 2 inlets, 11 outlets.	Microchannel width: 40 µm, height: 37 µm	Exosomes, microvesicles, apoptotic bodies (10^9 -10^{10}/mL). Sample flow rate: 50µL/hour. Sheath flow rate: 5000µL/hour.	>~90% separation efficiency of most extracellular vesicles (EV).	Size-selective separation and surface protein analysis of individual EVs.	Retention of individual EV via aptamer-mediated sorting into sheath buffer.	(Liu et al. 2019)
8	PDMS, glass, micropatterned electrodes.	Soft lithography, laser mask writing.	Two layers. 40 chambers (10×4), 1 inlet and 1 outlet. 4 flow channels. 5 pairs of electrodes.	Microchannel width: 30 µm, height: 70 µm, length: 7 mm.	5×10^5 cells/mL. 1.6mL/min.	Performance evaluated via successful electroporation of cells.	On-chip vortex-assisted electroporation system.	Electroporation device utilising inertial focusing.	(Ouyang et al. 2017)
9	Silicon wafers, PDMS.	Standard photolithography and casting.	High-aspect rectangular straight channel.	Microfluidic layer height 30 µm and width of 100 µm.	Sample flow rate: 70 µL/min and co-buffer flow rate: 140µL/min. 1000 cells/second.	96% buffer exchange efficiency.	Particle migration across streamlines, original research for RinSE device.	High-aspect channel.	(Gossett et al. 2012)
10	PDMS and glass.	Soft lithography, micromachining, moulding.	8-loop spiral microchannel architecture with trapezoidal cross-Sect. 1 inlet, 2 outlets.	Microchannel 600 µm width, 80 and 130 µm height (inner and outer wall heights respectively).	Average cell retention efficiency of 82% at a flow rate of 1mL/min per device.	IgG_1 recovery of up to 100%.	Novel cell-retention device for perfusion culture of mammalian cells.	Membrane-less cell retention system for harvesting of Ig-producing Chinese hamster ovary cells. Not a true buffer exchange device as cells are diluted externally.	(Kwon et al. 2017)
11	PDMS with glass.	Soft lithography.	Straight microchannels with two vortex-generating microchambers. 2 inlets and 4 outlets.	Microchannels have width of 30 µm and height of 50 µm. Microchambers have a dimension of 500 µm × 500 µm.	98–190µL/min. 23 µm beads: 700/mL, 18.5 µm: 1.8×10^4/mL.	Sorting of particles at 99% efficiency.	Continuous, size-based double sorting and purification of large target cells (away from smaller cells))	Particle separation causes larger particles to be exchanged into sheath flow.	(Wang et al. 2016)

Table 3 (continued)

Number	Device material(s)	Fabrication technique(s)	Microchannel architecture	Microchannel dimensions	Throughput	Performance	Application	Notes/ unique features	Reference
12	PDMS, SU8, glass, electrode.	Photolithography, micromoulding.	2 inlets, 5 outlets. Straight channels converging on a buffer swap region followed by serpentine channels into the dielectrophoresis region.	2 cm length, 1.5 cm width, 50 µm height.	Sheath flow: 129µL/min, sample inlet flow: 0.6µL/min. Sample outlet flow: 1.8µL/min. 3.88×10^8 cells/ml.	~99% buffer exchange.	Cell preparation prior to dielectrophoresis. On-chip solution exchange.	Transfers cells from physiological media to a lower conductivity medium.	(Huang et al. 2022)
N/A	PDMS, photoresist, silicon wafers.	Standard photolithograph, replica molding.	3 inlets converging onto one straight channel and 3 outlets.	1 cm length, 100 µm width, 30 µm height.	Sample flow: 35 µL/min, sheath flow: 140 µL/min.	100% solution exchange demonstrated.	Solution exchange of exosomes.	A tool used for affinity isolation of exosomes prior to detection via flow cytometry.	(Dudani et al. 2015)
Deterministic lateral displacement									
13	Silicon wafers, glass, polycarbonate, PDMS.	Deep reactive ion etching, soft lithography.	Varies. Micropost-containing channel, asymmetric curved, expansion channel for cell deflection	Varies throughout the device. Deflection channel is 500 µm wide, debulking channel is 150 µm in depth and distance between posts is 20–32 µm. Asymmetric channel was 52 µm in height.	~100 µL/min flow rate. Device performance evaluated at 200–1000 cells/mL of whole blood.	Capable of isolating circulating tumour cells at 0.1% purity (buffer exchange from whole blood to running buffer).	Cell sorting mediated through hydrodynamic size–dependent deterministic lateral displacement.	Buffer exchange was not the principle aim for the device.	(Ozkumur et al. 2013)

Table 3 (continued)

Number	Device material(s)	Fabrication technique(s)	Microchannel architecture	Microchannel dimensions	Throughput	Performance	Application	Notes/ unique features	Reference
14	Two module integrated device. Buffer exchange module: PDMS bonded to a layer of indium-tin-oxide (ITO) glass substrate. Optically induced electroporation module: hydrogen-rich amorphous-silicon-coated ITO glass with double-sided adhesive tape.	Bonding and stacked layers.	Straight channels with deterministic lateral displacement structures (microposts). Rectangular cross-sections.	Buffer exchange module: 30 μm diameter of microposts, 60 μm distance between microposts, channel height 50 μm. Electroporation module: 50 μm height. Channel width varies.	2.5×10^4 cells/minute with 10^6 cells/mL at a 25μL/min flow rate. 8.3% transfection efficiency demonstrated.	Solution exchange of culture medium with electroporation buffer.	The device is used for buffer exchange of human embryonic 293T cells (as exemplars) prior to optically-induced electroporation.	Integration of two modules.	(Lee et al. 2015)
15	DLD module: silicone gaskets, PDMS, SU-8. DEP module: patterning indium tin oxide electrodes and SU-8 well arrays. Glass and	DLD: Conventional photolithography, reactive-ion etching. DEP: Laser patterning and conventional photolithography.	Integrated DLD modules and DEP modules. 2 inlets, 2 outlets.	DLD module microchannel height: 60 μm, width: 2.5 mm. DEP module: diameter of the microwells: 24 μm, pitch: 100 μm. 5554 microwells in total. DEP microchannel width of 3.6 mm and the same height as DLD module.	Inlet 2 (buffer) at 1.5–2.5μL/min and outlets 1 and 2 both at 2μL/min pulling flow rate. Inlet 1 introduced sample via reservoir.	>~94% cells separated into alternative buffer. Successful buffer exchange verified through use of non-neat DEP buffer, demonstrating a reduction in performance.	The device uses DLD for medium exchange prior to analysis utilising DEP.	Prostate cancer cell trapping, separation and buffer exchange possible.	(Park et al. 2019)
Hydrodynamic filtration									
16	PDMS, glass.	Rapid prototyping using replica moulding	Straight channels. Three inlets, two waste drains, one outlet for recovery of cells.	Width of channels are variable (20–300 μm), height was uniform at 30 μm.	~1.3×10^6 cells/mL, up to maximum total flow rate of 140μL/min (with differing inlet flow rate ratios).	Rapid stimulation of cells with two stages of buffer exchange.	Extremely short chemical treatment of cells with a double solution exchange.	Cells undergo buffer exchange twice; one to a chemical-containing buffer and the second into a wash buffer.	(Yamada et al. 2008)

Table 3 (continued)

Number	Device material(s)	Fabrication technique(s)	Microchannel architecture	Microchannel dimensions	Throughput	Performance	Application	Notes/ unique features	Reference
17	Polyimide substrate, PMMA, PDMS, glass, SU-8.	Photolithography, soft lithography.	Hydrodynamic filtration and dielectrophoresis regions. 2 inlets, 3 outlets	Microchannel height: 75 µm, width at port channels: 1000 µm, channel width at electrodes: 3000 µm. Feeder width: 5 µm. Pillar dimensions: diameter (60 µm), pitch (140 µm), height (65 µm).	Both sample suspension and buffer injected at 30µL/min.	1×10^6 cell/mL. Near total buffer exchange capable for particles of cell relevant size (results displayed in terms of electrical conductivity). >90% efficiency.	Label-free target cell separation.	Jurkat cells.	(Oshiro et al. 2022)
Multistream laminar flow microfluidic cells									
N/A	Polystyrene coated glass with paraffin wax.	Custom technique (see method).	2 inlets,1 outlet. Straight channels.	1–3 mm narrow flow cells. 100 µm height.	7–200µL/min	Minimum exchange time of 0.25s.	Single-molecule reagent exchange.	Not cell based solution exchange.	(Madariaga-Marcos et al. 2020)
Dielectrophoresis									
18	PDMS with glass and electrodes.	Photolithography and soft lithography.	2 inlets, 2 outlets	Microchannel width: 500 µm and height 40 µm.	0.96µL/min minimal flow rate. Flow rate of 2µL/min mainly used.	3×10^6 cells/mL with medium exchange of 96.9%.	Automated medium exchange system capable of performing medium exchange at microvolumes.	The microchannel architecture contains a plane-stair shaped interdigital electrodes.	(Ma et al. 2021)
Acoustophoresis-based system									
19	Silicon and glass.	Deep reactive ion etching.	H shaped microchannel with 2 inlets and 2 outlets.	Microchannel width: 400 µm.	Typical flow rates of hundreds of µL/h to several mL/h.	10^6 cells/mL, with up to 84% of cells transferred between miscible fluids.	Solution exchange of cells or micro-sized particles.	Parasitic cells used.	(Liu et al. 2012)
20	Silicon wafer, glass, transducer attached.	Standard photolithography.	Straight channel, 1 sample inlet, 1 sample outlet. 8 buffer inlets and outlets.	Microchannel width: 375 µm, height: 150 µm, length: 6 cm.	80µL/min (sample inlet) with varying 25–40% of sample flow rate from buffer inlets.	$\sim5\times10^7$ particles or cells/mL, with 97% exchange.	Continuous buffer exchange of particle and cell suspensions.	Buffer exchange of more than 100% is possible due to wash buffer channels transversing the sample flow channel.	(Augustsson et al. 2009)

Table 3 (continued)

Number	Device material(s)	Fabrication technique(s)	Microchannel architecture	Microchannel dimensions	Throughput	Performance	Application	Notes/ unique features	Reference
21	Stainless steel, epoxy, composite transducer.	Laser cutting and layer bonding.	2 inlets connected to a main flow chamber and 2 outlets.	Chamber height: 375 µm, width: 17 mm.	10 mL/min total flow rate.	Whole blood used, > 80% exchange efficiency.	High throughput exchange of WBCs and RBCs.	Higher throughput and voltage of transducer was more efficient.	(Chen et al. 2016)
21	PMMA and piezoelectric plates.	Computer controlled cutting and engraving.	Straight channel, 1 sample inlet, 2 sheath flow inlets, 2 outlets.	Microchannel width: 1270 µm, depth: 500 µm.	Sheath flow: 20 and 200µL/min. Sample flow: 20µL/min.	Removal of 85–95% of platelets/WBC and RBC.	Isolation of platelet, WBC and RBC-depleted blood plasma.	Processing of undiluted whole blood.	(Ma et al. 2024)
Microfluidic device with integrated microwells									
22	PDMS with glass.	Photolithography and soft lithography	Layer with 5193 cylindrical microwells. Second flow layer.	Microwell diameter: 30 µm, depth: 100 µm. Flow channel of 200 µm depth.	Flow rate: 100µL/s.	6.2×10^5 – 1.6×10^7 cells/mL. 2000x reduction in concentration of fluorescent antibody	Multiple applications, including label-based separation of cells or solution exchange.	Not label-free but demonstrated use with donor leukocytes.	(Loutherback and Dietz 2022)
Continuous cross flow device									
23	PDMS, SU-8, silicon wafer, glass.	Photolithography, moulding and casting.	Two inlets and two outlets with a complex network of microchannels.	Microchannels with varying dimensions. Note: the authors recommend referring to the publication for further details.	0.21 and 0.60µL/min at sample and perfusion inlets, respectively.	98% of white blood cells retained with 4000-fold enrichment.	Separation of white blood cells from whole blood.	Continuous processing.	(VanDelinder and Groisman 2007)
'Centrifuge-on-a-Chip' device									
24	PDMS, KMPR 10–50, Mylar masks, glass.	Standard soft lithography and plasma bonding.	On-chip labelling required 3 inlets and 1 outlet, with 4 parallel flow channels.	Microchannel geometries vary depending on application. Generally, height: 70 µm, 40–50 µm width and 600–900 µm chamber size.	Flow rates of 2–4.4 mL/min.	1000 cells per chamber, solution exchange in 100ms.	Sample preparation device. Separation of cells, concentration of cells and solution exchange.	Only solution exchange data included.	(Mach et al. 2011)

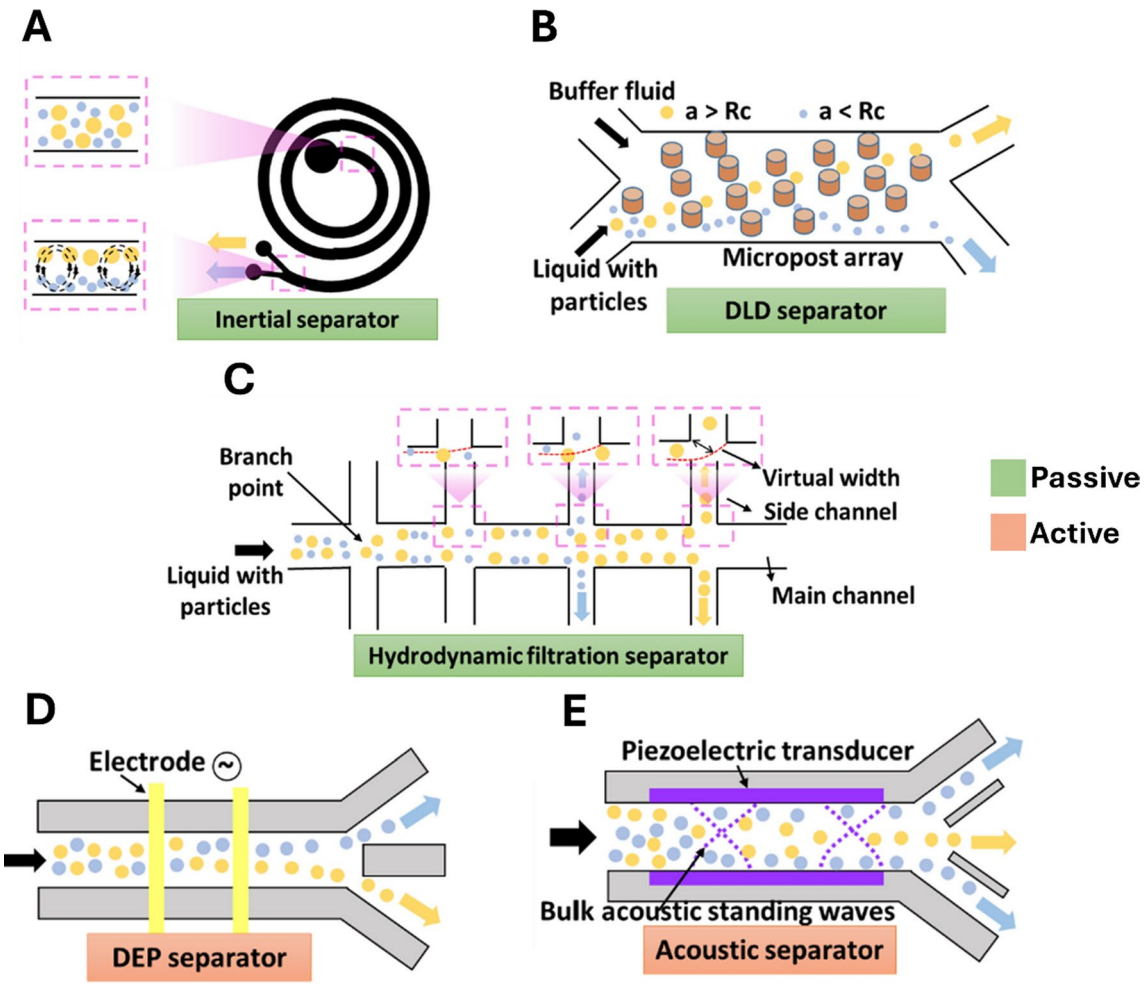

Fig. 3 Schematic diagram depicting different microfluidic techniques for separating particles and cells. **A**) Inertial focusing device with Dean flow, **B**) deterministic lateral displacement (DLD) device, **C**) hydrodynamic filtration device, **D**) dielectrophoresis (DEP) device and **E**) acoustophoresis device. The devices are further categorised as passive (red) or active (green) subtypes. Adapted from (Wu et al. 2023)

following buffer exchange to remove this excess and the device was used to achieve a cell suspension with up to 200 fold decrease in buffer conductivity (Huang et al. 2022).

An IF device with a high-aspect rectangular straight channel device processed labelled Michigan Cancer Foundation 7 cells (1000 cells/s) and investigated the capacity for solution transfer using the removal of unbound fluorescent labels to signify solution exchange. The label used was unnecessary for solution exchange but was used to demonstrate a capability to perform buffer exchange with 96% efficiency (Gossett et al. 2012). An IF device with an asymmetric curved channel used to prefocus cells prior to solution exchange in subsequent stages demonstrated removal of 95% of Eosin Y, a fluorescent dye used for cytoplasmic staining, from a suspension of cells (2×10^6 cell/mL, flow velocity 0.5 m/s) after four passages of the device (Reece et al. 2015).

Another group employed 3D-printing to produce an IF device with a 14-loop spiral architecture to automate buffer exchange via connection ports to a bioreactor and peristaltic pump. The device separated 95% of Chinese hamster ovary cells at a high throughput (2×10^7 cells/mL at 0.5-1.3mL/min) and recirculated these back to the bioreactor in a minimal volume (Enders et al. 2021), where fresh buffer could be added. This device utilised the largest number of spiral loops and was unique for 3D-printing manufacturing process, but had a low throughput that would require multiple parallelisation for large scale use in large bioreactors.

Some processes require the removal of certain nanoparticles from a suspension of cells and achieve this using gradient centrifugation. Tay et al., authored a protocol describing the design and manufacture a microfluidic device to replace the time-consuming conventional centrifuge-based process (Tay et al. 2016). The device utilises Dean flow fractionation in a spiral microchannel to remove 95% of free

fluorescent nanoparticles from a mixture of cells (maximum concentration 10^6 cells/mL) at a maximal flow rate of 1.5mL/min whilst recovering 90% of the cells. This device could perhaps be most useful as a downstream processing chip for removal of labels away from cells during previous cell processing.

An IF device with a straight channel was reported to be capable of processing up to 10^{10} extracellular vesicles (EVs)/mL at a flow rate of 5.5mL/hour (10:1, sheath flow: EV sample flow) with a separation efficiency of ~90%. Size-dependent separation caused EVs with a diameter < 200 nm to remain focused in the sample flow alongside DNA aptamers, but larger EVs behaved differently and were collected in sheath buffer at different outlets (Liu et al. 2019). This straight channel device was unique amongst IF-based buffer exchange devices as most utilised curvature of one form or another to mediate solution exchange.

Another highly efficient IF device is comprised of an 8-loop spiral microchannel with a trapezoidal cross-section. Under optimised flow conditions, the cross-section combined with the curvature caused Dean vortices to form off-centre focal positions and concentrated cells towards one outlet for volume reduction. These experiments were performed using high densities of cell suspensions ($> 2 \times 10^7$ cells/mL) with little evidence of channel clogging and so may be a good candidate for use in processing cells from bioreactors, despite requiring a second step to finish the buffer exchange process (Kwon et al. 2017).

One IF device contains a wavy microchannel and exploits elasto-inertial forces generated to separate a mixture of exosomes and large EVs achieving 81% separation of exosomes and large EVs collected in the sheath flow. Despite being smaller than cells and submicron in size, the separation of exosomes and large EVs remained possible due to the Dean vortices causing particle focusing due to the wavy geometry of the microchannel (Zhou et al. 2019).

Another IF device with spiral architecture processes dilute blood (10–15% haematocrit) at 5mL/minute with the goal of performing cell washing to remove immunoglobulin A (IgA) and other proteins. The device had a cell recovery equivalent to samples processed via conventional centrifugation but removed up to 10-fold more free protein from processed material. The IF device has a channel of 1.02 mm in diameter and so is technically beyond the microscale but as it utilises IF, it was included in this review (Vörös et al. 2018). This device therefore was unique in that it technically does not meet the usual specifications for inclusion as a microfluidic device but was listed due to the novel architecture and comparison with conventional centrifugation.

Other devices had a similar throughput and processed leukocytes at a concentration of 2×10^6 cells/min and flow rates of 15mL/min, but with a reported maximum of 60% buffer exchange efficiency (Carvell et al. 2024). This device had a particularly high rate of processing and whilst it was extremely efficient in cell separation, it had a relatively low efficiency of buffer exchange.

A rapid inertial device was reported to process exosomes for sample preparation prior to analysis by flow cytometry. This process previously required 5–7 centrifugation steps, and the use of the inertial device allows processing of exosomes in minutes, with a reported 100% solution exchange efficiency. Despite a simple manufacturing process, as the exosomes are sub-micron in size and the processing rate (~200µL/min) of the device is relatively low, this device is unlikely to be adopted for use in the processing of cell-sized analytes (Dudani et al. 2015).

These data show that IF devices are extremely capable of cell separation and performing adequate buffer exchange for a variety of processes and in particular, IF devices have a clear advantage in that they lack a need for labelling or an external force to manipulate cells. IF devices are suitable for performing buffer exchange for subsequent processes that are heavily dependent on correct buffer composition, as well as being capable of processing a range of targets of different sizes, ranging from sub-micron particles, EVS and larger cell types. IF devices in particular can be manufacturing relatively simply at the mass-production scale because they operate passively and require no additional integrated components.

5 Deterministic lateral displacement

As with IF, deterministic lateral displacement (DLD) is a label-free and passive microfluidic technique. It also separates cells based on size and shape and utilises flow channels with microstructures, commonly microposts, obstructing normal flow profiles and causing cells that reach a particular size threshold to flow out of microchannels perpendicular to the microstructures. In laminar flow, cells follow a streamline based on the position of the central region of the cell, but where microposts are located within this streamline, larger cells or particles are continually displaced into adjacent streamlines at each successive micropost. This is in contrast to smaller cells or particles which remain are capable of traversing the length of the microchannel within the original streamline following a zigzag profile (McGrath et al. 2014). DLD is label-free and a highly efficient method of bioprocessing and is capable of separating submicron-sized particles (Huang et al. 2004), but clogging remains a significant challenge to overcome (Salafi et al. 2019).

A device that employed DLD was used to facilitate continuous buffer exchange with two integrated modules for the solution exchange of culture medium to an electroporation

buffer. The device had a microchannel with a rectangular cross section with 60 µm distances between microposts and a complex system of microchannels that allowed processing of 2.5×10^4 cells/minute and a transfection efficiency of 8.3% following a successful buffer exchange (Lee et al. 2015). Another device that used DLD was employed to facilitate the buffer exchange of circulating tumour cells (CTCs) and white blood cells (WBCs) from blood into a running buffer fluid. Blood was injected alongside the running buffer and CTCs and WBCs were sorted through the micropost array into an asymmetric channel for IF to occur and before an expansion array (channel widening) chamber causes separation of CTCs (from 0.1% purity to allow for 99% detection in patients) and WBCs to different outlets. It is of note that this process relies on subsequent magnetically-labelling target CTCs and require a magnetic field for precise cell separation (Ozkumur et al. 2013).

Another multiple-module device utilised DLD arrays containing many pillars (diameter: 4 µm) with at least 30 µm gaps between each microstructure to separate a mixture of a prostate cancer cell line (5×10^5 cells/mL) and submicron-sized particles (3×10^9/mL) suspended in PBS. This device is unique because the flow within the main channel was largely driven via pulling at the outlets although flow is also pushed from the dielectrophoresis buffer inlet. The larger cells were separated from the tiny particles because the cells migrated in displacement mode through the pillar array, as opposed to the zigzag flow of the particles. This ensured the cells were exchanged continuously into coflowing dielectrophoresis buffer and were collected at an outlet for subsequent dielectrophoresis, whilst the particles remained within the original flow and were discarded at the waste outlet. Dielectrophoresis conductivity experiments showed that a buffer containing 2% phosphate buffered saline by volume alters the response relative to the dielectrophoresis buffer alone. At least 93% of cells were separated into the dielectrophoresis buffer and as the conductivity experiments showed processed cells were suspended in buffer with negligible differences in conductivity relative to neat dielectrophoresis buffer, indicating a near complete buffer exchange had been achieved (Park et al. 2019).

These data show that whilst DLD can be utilised for solution exchange and the devices discussed have demonstrated they are adequate for their respective applications, DLD devices are most likely not optimal for processing large volumes, or numbers, of cells. Furthermore, the complexities of manufacturing these devices makes them less ideal for adoption for mass production for simple buffer exchange in a wide range of cell-based bioprocessing applications.

6 Hydrodynamic filtration

Hydrodynamic filtration (HF) in microfluidics is a technique used to separate particles or cells based on their size, shape or other physical properties using fluid flow. HF uses microfluidic devices with a main flow microchannel and multiple branching side channels in which cells are collected. It is a label-free technique and functions by altering the flow rate of fluid at the inlets to generate certain flow conditions, where smaller cells behave differently from larger cells and have different focusing profiles at the cross-section of the microchannel. Through the design of appropriate side channel geometries, the smaller cells can be collected earlier in the flow and larger cells remain in the main channel for collection further downstream. The introduction of another fluid allows for buffer exchange and collection at target outlets (Aoki et al. 2009).

HF was utilised for the rapid buffer exchange of HeLa cells when cells require treatment with a reagent on the millisecond scale. The technique was used to flow cells at the inlet alongside a chemical reagent at a separate outlet whereby the cells underwent buffer exchange twice within hundreds of microseconds. The original cell suspension first was exchanged into Triton X-100 (a cell membrane solubilising reagent) and treated for ~40 microseconds before a wash buffer at higher flow rate caused a re-exchange of cells out of the Triton X-100 and therefore allowed for a limited and rapid exposure to the cell membrane-damaging reagent (Yamada et al. 2008). In one device, two modules sorted Jurkat and MCF7 cells (both $\sim 2.5 \times 10^5$ cells/mL) based on HF for buffer exchange before the active component utilises dielectrophoresis for final cell separation. Mixed cell samples (of different sizes) were injected at one inlet alongside dielectrophoresis buffer at the other inlet. As the samples reached the HF region, the smaller cells were removed from the flow through side channels and larger target cells proceeded to the dielectrophoresis module where the electric separation of target and non-target cells was performed. The efficiency of buffer exchange was evaluated based on conductivity of the fluid and there was a reduction from 1000 mS/m to ~35 mS/m, similar to that of dielectrophoresis buffer, indicating a successful buffer exchange was performed (Oshiro et al. 2022). Whilst this device using HF demonstrated good efficiency of buffer exchange, it is unclear how this device could be utilised for solution exchange on an industrial scale as it is comprised of two device components and the associated manufacturing costs could limit this device for research purposes only.

7 Dielectrophoresis

Dielectrophoresis can also be employed alongside microfluidic technologies to perform buffer exchange, but it differs from IF, DLD and HF because although is label-free, it uses a non-uniform electric field and therefore is not considered a passive microfluidic technology. Polarisable cells and particles within the fluid flow experience forces that arise between the gradient of the electric field and the induced dipole moment in the cells (or particles) and these forces are capable of manipulating cells and causing an exchange from fluid to fluid. This process requires precise control and optimisation of electrical frequencies, cell concentration and microchannel architecture (Sarno et al. 2021).

An automatic medium exchange device that employed dielectrophoresis to directly force cells from the cell suspension to a fresh culture medium was reported with ~97% harvest efficiency within microvolumes of culture. The process is fully automated and uses plane stair-shaped interdigital electrodes to generate the electric field within laminar flow and facilitate the continuous buffer exchange process. This device used relatively concentrated cell suspensions and was capable of exchanging the buffer of 3×10^6 HeLa cells/mL albeit at a low flow rate of 2µL/min meaning it may only be suitable for smaller volumes of cells or would require massive parallelisation (Ma et al. 2021).

8 Acoustophoresis

Microfluidic devices using acoustophoresis are arguably more similar to those employing dielectrophoresis than IF or DLD alone because, like dielectrophoresis, they utilise forces that arise as a result of the function of electrical components. The acoustophoresis of cells is achieved by leveraging acoustic forces generated when the forces interact with the fluid medium around the cells within the microchannel. It is the complex interactions between the hydrodynamic forces generated by the fluid flow within the device and the acoustic forces produced by the device transducer that allow operators to manipulate cells from fluid to fluid (Wu et al. 2019).

One microfluidic device uses ultrasonic standing waves to manipulate cells and induce buffer exchange of erythrocyte suspensions. This device contained a straight channel fed via one sample inlet and outlet, and 8 buffer inlets and outlets. The buffer channels were orientated nearly perpendicular to the main flow channel and were downstream of the acoustically active portion of the flow channel that enabled cell focusing into a streamline. The device was capable of processing 5×10^7 cells/mL with a sample inlet flow rate of 80µL/min and achieved 97% buffer exchange efficiency. It is of note that this device is technically capable of greater than 100% buffer exchange due to multiple wash channels transversing the flow channel (Augustsson et al. 2009). Another microfluidic device utilising an H-shaped flow channel and acoustophoresis for buffer exchange was capable of processing 10^6 cells/mL at widely ranging flow rates (hundreds of µL/hr - hundreds of mL/hr) and achieved up to 84% transfer of waterborne unicellular parasites between two fluids during the processing. Although diffusion between fluids was observed, there was negligible impact on any of the required processes in this buffer exchange step and would be unlikely to affect post-processing applications (Liu et al. 2012).

A high-throughput acoustic device was reported to separate up to 80% of platelets from red blood cells (RBCs) and white blood cells (WBCs) from whole blood at a throughput of 10 mL/min. This was performed by flowing buffer and whole blood over a transducer within the fluid chamber and the platelets are sorted to the lower outlet whereas the RBCs and WBCs are exchanged into a phosphate-buffered solution and collected at the upper outlet due the larger cell volumes of the RBCs and WBCs relative to the platelets. This device has relatively good separation efficiency and biocompatibility, but excellent throughput and would be useful for processing of whole blood with the aim to enrich WBCs, RBCs or alternatively platelets (Chen et al. 2016).

A more recent study utilising a device that purposefully introduces acoustic impedance alongside acoustic radiation force and demonstrated a capacity to remove platelets, WBCs and RBCs from whole blood, enabling blood plasma to be captured in a label-free process. The device, comprised of PMMA and piezoelectric modules, removed > 90% of non-target cells at a flow rate of 20 µL/min. Whilst the throughput is lower than reported in other devices, this acoustofluidic device has the potential for continuous processing of undiluted whole blood and removes non-target cells with minimal post-processing effects on protein expression and therefore may be a useful diagnostic tool in the future (Ma et al. 2024).

9 Other microfluidic devices

There are several unique microfluidic devices designed for buffer exchange within biotechnologies and a selection are listed below.

9.1 Multi-stream laminar flow

A multi-stream laminar flow device was designed with a main flow channel supplied via two inlets and leading to a single outlet. The device is flexible with regard to application and was predominantly used for reagent exchange for single

molecule studies, including oligonucleotides. The device is capable of buffer exchange because it utilises a non-mixing laminar flow regime with variable inlet flow rates that alters the proportions of fluid occupancy within the microchannel. By decreasing the flow rate at one inlet, the relatively high flow rate inlet fluid occupies most of the main flow channel, thereby ensuring the molecule is contained within the high flow inlet fluid. Through the image analysis of the microchannel to determine the concentration of fluorescein, a fluorescent dye used to stain cells for tracking in microscopy, the capacity of the multi-stream laminar flow device for buffer exchange was determined. A near 100% buffer exchange was possible with a fluid switch time of approximately one hundred microseconds, making the device a low-cost and highly attractive candidate for the efficient buffer exchange for single-molecule studies (Madariaga-Marcos et al. 2020). However, it should be noted that this multi-stream device approach was demonstrated for molecules and not cells unlike the other devices described in this review.

9.2 Microwells

A microfluidic device with integrated microwells has demonstrated a capability to perform buffer exchange of donor leukocytes, without using centrifugation, over approximately 40 min. Peripheral blood mononuclear cells were labelled with immunomagnetic particles and perfused over the top of the well layer. Human CD14 + monocyte cells were captured by utilising immunomagnetic isolation via strong magnets orientated proximal to the ~5000 wells with the non-target cells being flushed out in the subsequent wash process. The second wash step at 1µL/s was used to remove unbound label from the wells and the magnets were removed to allow the target cells to flow out of the wells into the main flow channel. This device requires the use of a label and is quite low throughput but benefits from avoiding centrifugation and pelletisation of the cells which can cause damage to cell membranes. This is main advantage of this technique as it may be gentler to isolate and buffer exchange due to the low forces experienced by microwell capture relative to processes involving centrifugation (Loutherback and Dietz 2022).

9.3 Continuous cross flow

A microfluidic device utilising continuous cross flow reported the ability to separate white blood cells (WBCs) from whole blood. There were two inlets where whole blood and a perfusion medium was injected and two outlets to collect purified WBCs and waste, respectively. The main flow channel was flanked by a system of buffer perfusion channels and a complementary system of buffer extraction channels. As whole blood flowed through the main channel, perfusion buffer flowed perpendicularly through hundreds of increasingly smaller channels, and smaller red blood cells were washed out of the main channel. Following processing, the outlet sample had a 4000-fold reduced concentration of red blood cells whilst retaining nearly all WBCs (98%), in comparison to the whole blood at the inlet. The device had very good separation and buffer exchange capacity but very low throughput, with a blood inlet flow rate of ~50µL/minute and haematocrit of ~40% (VanDelinder and Groisman 2007).

Table 3 lists different microfluidic devices capable of buffer exchange of cells or molecules and used for bioprocessing applications. The list is not exhaustive but aims to be a referral tool for which researchers can use to help determine how future devices can be designed and for comparisons for the evaluation of the performance of future devices.

9.4 Vortex-trapping assisted solution exchange

A microfluidic device was designed to replace the basic processes performed by centrifugation. This device utilises microvortices to selectively trap cells and has demonstrated an ability to enrich rare cancer cells from spiked blood samples at relatively high throughput. The device is capable of performing solution exchange by first processing the sample fluid, trapping the cells within vortices in the flow, followed by injection of a separate buffer at the inlet to displace the sample fluid and perform complete solution exchange of the cells with minimal cell loss (Mach et al. 2011).

10 Conclusion

Microfluidic devices represent a significant advancement in the field of buffer exchange, offering precise, efficient, and scalable solutions. These devices leverage the principles of fluid dynamics at the microscale, enabling the manipulation of small volumes of fluids with high accuracy. The diverse range of microfluidic devices available caters to various applications and may utilise labels or forces generated by electrical components or simply operate passively based on the hydrodynamic forces generated by the microchannel architecture. There is huge flexibility in design which allows for a wide range of applications and as such various microfluidic devices are promising candidates to perform buffer exchange in biotechnologies in the future. This review supports the conclusion that IF devices used for buffer exchange had the highest throughput in terms of processing rates, especially those devices with spiral microchannel geometries. However, not all IF devices were optimal and whilst some had near 100% buffer exchange efficiency,

others had a limited throughput and performed poorly with regard to buffer exchange. Most devices operated in a label-free manner but the devices that required the use of labels all exceeded 90% efficiency of buffer exchange. Label free processing is advantageous because it would allow for continual processing without the addition of GMP-compliant reagents, but passive cell manipulation in processes such as IF require a relatively uniform size and shape of cellular material. Some of the most efficient devices utilised external forces, such as dielectrophoresis and acoustophoresis, but are again limited with respect to their processing rates. Those that used electrical components, for example, were primarily designed for buffer exchange at a small volume, using a relatively small number of cells, for upstream processing activities such as electroporation and as such, these devices may be more suited for research applications. An absence of external forces is desirable for bioprocessing as it not only reduces design and manufacturing complexities, but also ensures that integration of massively parallelised devices will not be hampered by the device design requiring components throughout the product after scale-up. Despite some remaining technical challenges such as channel clogging, buffer exchange through microfluidic device processing remains a viable and attractive option when compared with conventional processing methods.

Author contributions Conceptualisation: TC; Writing - original draft preparation: TC; Writing - review and editing: TC, HB, AF, PB.

Funding This work was supported by Medical Research Scotland (grant no. 50167 – 2019) and internal research funding from NHS National Services Scotland.

Data availability Data for Fig. 2 is provided within an excel file and is available for download here: https://figshare.com/articles/figure/Data_for_figure_2/27089314?file=49365952.

Declarations

Competing interests The authors declare no competing interests.

Declaration of AI use We declare we have not used AI-assisted technologies in creating this article.

References

Amini H, Lee W, Di Carlo D (2014) Inertial microfluidic physics. Lab Chip 14(15):2739–2761. https://doi.org/10.1039/C4LC00128A

Aoki R, Yamada M, Yasuda M, Seki M (2009) In-channel focusing of flowing microparticles utilizing hydrodynamic filtration. Microfluid Nanofluid 6(4):571–576. https://doi.org/10.1007/s10404-008-0334-0

Augustsson P, Åberg LB, Swärd-Nilsson A-MK, Laurell T (2009) Buffer medium exchange in continuous cell and particle streams using ultrasonic standing wave focusing. Microchim Acta 164(3):269–277. https://doi.org/10.1007/s00604-008-0084-4

Bahnemann J, Grünberger A (2022) Microfluidics in Biotechnology: overview and Status Quo. Adv Biochem Eng Biotechnol 179:1–16. https://doi.org/10.1007/10_2022_206

Battat S, Weitz DA, Whitesides GM (2022) An outlook on microfluidics: the promise and the challenge. Lab Chip 22(3):530–536. https://doi.org/10.1039/d1lc00731a

BioSep (2020) BioSep, Acoustic cell retention system. In

Brown C, McKee C, Bakshi S, Walker K, Hakman E, Halassy S, Chaudhry GR (2019) Mesenchymal stem cells: cell therapy and regeneration potential. J Tissue Eng Regen Med 13(9):1738–1755. https://doi.org/10.1002/term.2914

Calmels B, Houzé P, Hengesse JC, Ducrot T, Malenfant C, Chabannon C (2003) Preclinical evaluation of an automated closed fluid management device: Cytomate, for washing out DMSO from hematopoietic stem cell grafts after thawing. Bone Marrow Transpl 31(9):823–828. https://doi.org/10.1038/sj.bmt.1703905

Carvell T, Burgoyne P, Milne L, Campbell JDM, Fraser AR, Bridle H (2024) Human leucocytes processed by fast-rate inertial microfluidics retain conventional functional characteristics. J R Soc Interface 21(212):20230572. https://doi.org/10.1098/rsif.2023.0572

Chen Y, Wu M, Ren L, Liu J, Whitley PH, Wang L, Huang TJ (2016) High-throughput acoustic separation of platelets from whole blood. Lab Chip 16(18):3466–3472. https://doi.org/10.1039/C6LC00682E

Convery N, Gadegaard N (2019) 30 years of microfluidics. Micro Nano Eng 2:76–91. https://doi.org/10.1016/j.mne.2019.01.003

Cooper RS, Sutherland C, Smith LM, Cowan G, Barnett M, Mitchell D, Fraser AR (2024) EBV T-cell immunotherapy generated by peptide selection has enhanced effector functionality compared to LCL stimulation. Front Immunol 15:1412211. https://doi.org/10.3389/fimmu.2024.1412211

Cossarizza A, Chang H-D, Radbruch A, Akdis M, Andrä I, Annunziato F, Zimmermann J (2017) Guidelines for the use of flow cytometry and cell sorting in immunological studies. Eur J Immunol 47(10):1584–1797. https://doi.org/10.1002/eji.201646632

Delahaye M, Lawrence K, Ward SJ, Hoare M (2015) An ultra scale-down analysis of the recovery by dead-end centrifugation of human cells for therapy. Biotechnol Bioeng 112(5):997–1011. https://doi.org/10.1002/bit.25519

Dudani JS, Gossett DR, Tse HT, Lamm RJ, Kulkarni RP, Carlo DD (2015) Rapid inertial solution exchange for enrichment and flow cytometric detection of microvesicles. Biomicrofluidics 9(1):014112. https://doi.org/10.1063/1.4907807

El-Kadiry AE-H, Rafei M, Shammaa R (2021) Cell therapy: types, regulation, and clinical benefits. Front Med 8. https://doi.org/10.3389/fmed.2021.756029

Elverum K, Whitman M (2020) Delivering cellular and gene therapies to patients: solutions for realizing the potential of the next generation of medicine. Gene Ther 27(12):537–544. https://doi.org/10.1038/s41434-019-0074-7

Enders A, Preuss JA, Bahnemann J (2021) 3D printed microfluidic spiral separation device for continuous, Pulsation-Free and

controllable CHO cell Retention. Micromachines (Basel) 12(9). https://doi.org/10.3390/mi12091060
Gossett DR, Tse HT, Dudani JS, Goda K, Woods TA, Graves SW, Di Carlo D (2012) Inertial manipulation and transfer of microparticles across laminar fluid streams. Small 8(17):2757–2764. https://doi.org/10.1002/smll.201200588
Gou Y, Jia Y, Wang P, Sun C (2018) Progress of Inertial Microfluidics in Principle and Application. Sensors 18(6):1762. https://doi.org/10.3390/s18061762
Guzniczak E, Otto O, Whyte G, Willoughby N, Jimenez M, Bridle H (2020) Deformability-induced lift force in spiral microchannels for cell separation. Lab Chip 20(3):614–625. https://doi.org/10.1039/c9lc01000a
Huang LR, Cox EC, Austin RH, Sturm JC (2004) Continuous particle separation through deterministic lateral displacement. Science 304(5673):987–990. https://doi.org/10.1126/science.1094567
Huang D, Man J, Jiang D, Zhao J, Xiang N (2020) Inertial microfluidics: recent advances. Electrophoresis. https://doi.org/10.1002/elps.202000134
Huang X, Torres-Castro K, Varhue W, Rane A, Rasin A, Swami NS (2022) On-chip microfluidic buffer swap of biological samples in-line with downstream dielectrophoresis. Electrophoresis 43(12):1275–1282. https://doi.org/10.1002/elps.202100304
Ibenana L, Anderson R, Gee A, Gilbert M, Cox C, Hare JM, McKenna DH (2022) Assessment of the LOVO device for final harvest of novel cell therapies: a production assistance for Cellular therapies multi-center study. Cytotherapy 24(7):691–698. https://doi.org/10.1016/j.jcyt.2022.01.010
Iwama A, Hirayama J, Nogawa M, Shiba M, Satake M, Takamoto S, Tadokoro K (2017) Comparison between in vitro properties of washed platelet concentrates suspended in M-sol and those in BRS-A, both of which were prepared with an automated cell processor. Transfus Apheres Sci 56(2):241–244. https://doi.org/10.1016/j.transci.2017.01.007
Kalyan S, Torabi C, Khoo H, Sung HW, Choi S-E, Wang W, Hur SC (2021) Inertial Microfluidics Enabling Clinical Research. *Micromachines, 12*(3), 257. Retrieved from https://www.mdpi.com/2072-666X/12/3/257
Kersaudy-Kerhoas M, Sollier E (2013) Micro-scale blood plasma separation: from acoustophoresis to egg-beaters. Lab Chip 13(17):3323–3346. https://doi.org/10.1039/c3lc50432h
Koo EH (2024) Current state of endothelial cell therapy. Curr Opin Ophthalmol 35(4):304–308. https://doi.org/10.1097/icu.0000000000001050
Kurnik RT, Yu AW, Blank GS, Burton AR, Smith D, Athalye AM, van Reis R (1995) Buffer exchange using size exclusion chromatography, countercurrent dialysis, and tangential flow filtration: models, development, and industrial application. Biotechnol Bioeng 45(2):149–157. https://doi.org/10.1002/bit.260450209
Kwon T, Prentice H, Oliveira J, Madziva N, Warkiani ME, Hamel JP, Han J (2017) Microfluidic Cell Retention device for perfusion of mammalian suspension culture. Sci Rep 7(1):6703. https://doi.org/10.1038/s41598-017-06949-8
Lee G-B, Chang C-J, Wang C-H, Lu M-Y, Luo Y-Y (2015) Continuous medium exchange and optically induced electroporation of cells in an integrated microfluidic system. Microsystems Nanoengineering 1(1):15007. https://doi.org/10.1038/micronano.2015.7
Li A, Wilson S, Fitzpatrick I, Chan S, Barabadi M, Kusuma G, Lim R (2019) Evaluating automated buffer exchange protocols using Rotea™ counterflow centrifuge. Cytotherapy 21(5). https://doi.org/10.1016/j.jcyt.2019.03.379
Li A, Kusuma GD, Driscoll D, Smith N, Wall DM, Levine BL, Lim R (2021) Advances in automated cell washing and concentration. Cytotherapy 23(9):774–786. https://doi.org/10.1016/j.jcyt.2021.04.003
Liu Y, Hartono D, Lim KM (2012) Cell separation and transportation between two miscible fluid streams using ultrasound. Biomicrofluidics 6(1):12802–1280214. https://doi.org/10.1063/1.3671062
Liu C, Zhao J, Tian F, Chang J, Zhang W, Sun J (2019) λ-DNA- and aptamer-mediated sorting and analysis of Extracellular vesicles. J Am Chem Soc 141(9):3817–3821. https://doi.org/10.1021/jacs.9b00007
Loutherback K, Dietz AB (2022) Capture and reagent exchange (CARE) wells for cell isolation, labeling, and characterization. Microfluid Nanofluid 26(8):60. https://doi.org/10.1007/s10404-022-02568-6
Lu M, Lezzar DL, Vörös E, Shevkoplyas SS (2019) Traditional and emerging technologies for washing and volume reducing blood products. J Blood Med 10:37–46. https://doi.org/10.2147/jbm.S166316
Lu R-M, Hwang Y-C, Liu IJ, Lee C-C, Tsai H-Z, Li H-J, Wu H-C (2020) Development of therapeutic antibodies for the treatment of diseases. J Biomed Sci 27(1):1. https://doi.org/10.1186/s12929-019-0592-z
Ma Z, Zhao H, Shi L, Yu D, Guo X (2021) Automatic medium exchange for micro-volume cell samples based on dielectrophoresis. Electrophoresis 42(14–15):1507–1515. https://doi.org/10.1002/elps.202000195
Ma Z, Xia J, Upreti N, David E, Rufo J, Gu Y, Huang TJ (2024) An acoustofluidic device for the automated separation of platelet-reduced plasma from whole blood. Microsystems Nanoengineering 10(1):83. https://doi.org/10.1038/s41378-024-00707-3
Mach AJ, Kim JH, Arshi A, Hur SC, Di Carlo D (2011) Automated cellular sample preparation using a centrifuge-on-a-Chip. Lab Chip 11(17):2827–2834. https://doi.org/10.1039/C1LC20330D
Madariaga-Marcos J, Corti R, Hormeño S, Moreno-Herrero F (2020) Characterizing microfluidic approaches for a fast and efficient reagent exchange in single-molecule studies. Sci Rep 10(1):18069. https://doi.org/10.1038/s41598-020-74523-w
Martel JM, Toner M (2014) Inertial focusing in Microfluidics. Annu Rev Biomed Eng 16(1):371–396. https://doi.org/10.1146/annurev-bioeng-121813-120704
Masri F, Hoeve M, Sousa P, Willoughby N (2017) Challenges and advances in scale-up of label-free downstream processing for allogeneic cell therapies. Cell Gene Therapy Insights 3:447–467. https://doi.org/10.18609/cgti.2017.041
McGrath J, Jimenez M, Bridle H (2014) Deterministic lateral displacement for particle separation: a review. Lab Chip 14(21):4139–4158. https://doi.org/10.1039/C4LC00939H
Moroni F, Dwyer BJ, Graham C, Pass C, Bailey L, Ritchie L, Forbes SJ (2019) Safety profile of autologous macrophage therapy for liver cirrhosis. Nat Med 25(10):1560–1565. https://doi.org/10.1038/s41591-019-0599-8
Myers JA, Miller JS (2021) Exploring the NK cell platform for cancer immunotherapy. Nat Rev Clin Oncol 18(2):85–100. https://doi.org/10.1038/s41571-020-0426-7
Oikawa S, Minegishi M, Endo K, Kawashima W, Suzuki K, Shimizu H (2016) Washing of platelets can be fully automated using a closed-system cell processor and BRS-A platelet additive solution. Vox Sang 111(4):437–440. https://doi.org/10.1111/vox.12439
Oshiro K, Wakizaka Y, Takano M, Itoi T, Ohge H, Koba K, Maruyama F (2022) Fabrication of a new all-in-one microfluidic dielectrophoresis integrated chip and living cell separation. iScience 25(2):103776. https://doi.org/10.1016/j.isci.2022.103776
Ouyang M, Hill W, Lee JH, Hur SC (2017) Microscale Symmetrical Electroporator array as a versatile Molecular Delivery System. Sci Rep 7(1):44757. https://doi.org/10.1038/srep44757
Ozkumur E, Shah AM, Ciciliano JC, Emmink BL, Miyamoto DT, Brachtel E, Toner M (2013) Inertial focusing for tumor antigen-dependent and -independent sorting of rare circulating tumor

cells. Sci Transl Med 5(179):179ra147. https://doi.org/10.1126/scitranslmed.3005616
Park J, Komori T, Uda T, Miyajima K, Fujii T, Kim SH (2019) Sequential cell-Processing System by integrating Hydrodynamic purification and dielectrophoretic trapping for analyses of suspended Cancer cells. Micromachines (Basel) 11(1). https://doi.org/10.3390/mi11010047
Pritchard RH, Zhukov AA, Fullerton JN, Want AJ, Hussain F, la Cour MF, Rogers SS (2019) Cell sorting actuated by a microfluidic inertial vortex. Lab Chip 19(14):2456–2465. https://doi.org/10.1039/C9LC00120D
Ramachandraiah H, Ardabili S, Faridi AM, Gantelius J, Kowalewski JM, Mårtensson G, Russom A (2014) Dean flow-coupled inertial focusing in curved channels. Biomicrofluidics 8(3):034117. https://doi.org/10.1063/1.4884306
Reece AE, Kaastrup K, Sikes HD, Oakey J (2015) Staged Inertial Microfluidic focusing for Complex Fluid Enrichment. RSC Adv 5:53857–53864. https://doi.org/10.1039/c5ra10634f
Roddie C, O'Reilly M, Dias Alves Pinto J, Vispute K, Lowdell M (2019) Manufacturing chimeric antigen receptor T cells: issues and challenges. Cytotherapy 21(3):327–340. https://doi.org/10.1016/j.jcyt.2018.11.009
Salafi T, Zhang Y, Zhang Y (2019) A review on deterministic lateral displacement for particle separation and detection. Nanomicro Lett 11(1):77. https://doi.org/10.1007/s40820-019-0308-7
Sarno B, Heineck D, Heller MJ, Ibsen SD (2021) Dielectrophoresis: developments and applications from 2010 to 2020. Electrophoresis 42(5):539–564. https://doi.org/10.1002/elps.202000156
Starkey Lewis PJ, Moroni F, Forbes SJ (2019) Macrophages as a cell-based therapy for Liver Disease. Semin Liver Dis 39(4):442–451. https://doi.org/10.1055/s-0039-1688502
Sutermaster BA, Darling EM (2019) Considerations for high-yield, high-throughput cell enrichment: fluorescence versus magnetic sorting. Sci Rep 9(1):227. https://doi.org/10.1038/s41598-018-36698-1
Tay HM, Yeo DC, Wiraja C, Xu C, Hou HW (2016) Microfluidic Buffer Exchange for interference-free Micro/Nanoparticle Cell Engineering. J Vis Exp 113. https://doi.org/10.3791/54327
Tomlinson MJ, Tomlinson S, Yang XB, Kirkham J (2013) Cell separation: terminology and practical considerations. J Tissue Eng 4:2041731412472690. https://doi.org/10.1177/2041731412472690
VanAernum ZL, Busch F, Jones BJ, Jia M, Chen Z, Boyken SE, Wysocki VH (2020) Rapid online buffer exchange for screening of proteins, protein complexes and cell lysates by native mass spectrometry. Nat Protoc 15(3):1132–1157. https://doi.org/10.1038/s41596-019-0281-0
VanDelinder V, Groisman A (2007) Perfusion in Microfluidic Cross-flow: separation of White Blood cells from whole blood and exchange of medium in a continuous Flow. Anal Chem 79(5):2023–2030. https://doi.org/10.1021/ac061659b
Vormittag P, Gunn R, Ghorashian S, Veraitch FS (2018) A guide to manufacturing CAR T cell therapies. Curr Opin Biotechnol 53:164–181. https://doi.org/10.1016/j.copbio.2018.01.025
Vörös E, Piety NZ, Strachan BC, Lu M, Shevkoplyas SS (2018) Centrifugation-free washing: a novel approach for removing immunoglobulin A from stored red blood cells. Am J Hematol 93(4):518–526. https://doi.org/10.1002/ajh.25026
Wang X, Yang X, Papautsky I (2016) An integrated inertial microfluidic vortex sorter for tunable sorting and purification of cells. TECHNOLOGY 04(02):88–97. https://doi.org/10.1142/s2339547816400112
Weber EW, Maus MV, Mackall CL (2020) The Emerging Landscape of Immune Cell therapies. Cell 181(1):46–62. https://doi.org/10.1016/j.cell.2020.03.001
Wu M, Ozcelik A, Rufo J, Wang Z, Fang R, Jun Huang T (2019) Acoustofluidic separation of cells and particles. Microsystems Nanoengineering 5(1):32. https://doi.org/10.1038/s41378-019-0064-3
Wu J, Fang H, Zhang J, Yan S (2023) Modular microfluidics for life sciences. J Nanobiotechnol 21(1):85. https://doi.org/10.1186/s12951-023-01846-x
Yamada M, Kobayashi J, Yamato M, Seki M, Okano T (2008) Millisecond treatment of cells using microfluidic devices via two-step carrier-medium exchange. Lab Chip 8:772–778. https://doi.org/10.1039/b718281c
Yang Y, Rao R, Valliere-Douglass J, Tremintin G (2024) Automated high-throughput buffer exchange platform enhances rapid flow analysis of antibody drug conjugates by high resolution mass spectrometry. J Chromatogr B 1235:124007. https://doi.org/10.1016/j.jchromb.2024.124007
Zhou Y, Ma Z, Tayebi M, Ai Y (2019) Submicron Particle Focusing and Exosome sorting by Wavy Microchannel structures within viscoelastic fluids. Anal Chem 91(7):4577–4584. https://doi.org/10.1021/acs.analchem.8b05749